



King Saud University
Arabian Journal of Chemistry

www.ksu.edu.sa
www.sciencedirect.com



ORIGINAL ARTICLE

1st Nano Update

Kinetics of silver nanoparticle growth in aqueous polymer solutions

Zaheer Khan ^{a,b,*}, Shael Ahmed Al-Thabaiti ^a, F.M. Al-Nowaiser ^a,
Abdullah Yousif Obaid ^a, Abdulrahman O. Al-Youbi ^a, Maqsood Ahmad Malik ^b

^a Department of Chemistry, Faculty of Science, King Abdul Aziz University, P.O. Box 80203, Jeddah 21413, Saudi Arabia

^b Department of Chemistry, Jamia Millia Islamia (Central University), New Delhi 110 025, India

Received 18 August 2010; accepted 27 December 2010

Available online 30 December 2010

KEYWORDS

Nanoparticles;
Polymer;
Citric acid;
Surfactant

Abstract In this paper we report the effect of poly(vinyl alcohol) (PVA) on the silver nanoparticles formation of different morphologies by using silver nitrate and citric acid as the oxidant and reductant, respectively, for the first time. Our transmission electron microscopy (TEM) results suggest that the presence of PVA has significant impact on the size, shape, and the size distribution of the silver nanoparticles. The reaction follows a zero-order kinetics in [citric acid] as well as in [silver(I)] in the absence and presence of PVA. It was found that PVA and cetyltrimethylammonium bromide (CTAB) concentrations show no significant effects on the rate of CTAB-stabilized silver nanoparticles formation, whereas in presence of PVA, the reaction rate increases with (CTAB). Both spectrophotometric and TEM measurement demonstrated that the orange silver sol consists of aggregates, whereas the purple sol does not contain the aggregated arrangement. On the basis of various observations, the most plausible mechanism has been envisaged.

© 2011 King Saud University. Production and hosting by Elsevier B.V. All rights reserved.

* Corresponding author at: Department of Chemistry, Jamia Millia Islamia (Central University), New Delhi 110 025, India. Tel.: +91 11 26981717.

E-mail address: drkhanchem@yahoo.co.in (Z. Khan).

1878-5352 © 2011 King Saud University. Production and hosting by Elsevier B.V. All rights reserved.

Peer review under responsibility of King Saud University.
doi:10.1016/j.arabjc.2010.12.024



Production and hosting by Elsevier

1. Introduction

Formation and characterization of silver nanoparticles with different shape and size by a large number of methods (chemical, radiation, photo and electrochemical) with and without stabilizers (surfactants, polymers, copolymers, long chain unsaturated carboxylates, solid matrix, and hyperbranched dendrimers) have been the subject of a large number of investigators for a long time (Henglein, 1993; Pileni, 1993; Pal et al., 1997; Ball, 1991; Wang et al., 1999; Sondi et al., 2003; Mayer et al., 2000; Keki et al., 2000; Saito et al., 1996; Kim et al.,

2009). Generally, sodium citrate, ascorbic acid, sodium borohydride, and hydrazine have been used for the preparation of these nanomaterials by chemical reduction of silver ions (Lee and Meisel, 1982; Kamat et al., 1998; Jana et al., 1999; Zhai and Efrima, 1996; Al-Thabaiti et al., 2008). It is well known that the most important role of the stabilizing agents is to protect the nanoparticles from coagulation. Preparation of silver nanoparticles by different oxidizing agents is of special importance due to their biocidal and non-toxic relevance. Surfactants role in bulk solution and at interfaces is of great importance in surface chemistry. Surfactants properties have attracted growing attention for use in biological and chemical research applications. The colloidal solutions of nanometer particles has been found advantageous over the water insoluble forms (e.g., enhanced catalytic and oxidizing activities – due to large specific surface area – and possibility of monitoring reactions by UV–vis spectrophotometry).

Henglein (Henglein, 1998) reported the capping action of citrate in the formation of long-time stable colloidal silver nanoparticles by the radiation method (citrate is solely a spectator to the ongoing redox processes). The role of polymers in the size, shape, and the size distribution of the silver nanoparticle formation is well-documented in the literature (Henglein, 1993, 1998; Huang et al., 1996; Lee et al., 2002; Suber et al., 2005; Bakar et al., 2007) but the systematic kinetics of the silver sol formation is rare in the similar studies (Patakfalvi et al., 2004). Recently, we have discussed the mechanism of Ag-nanoparticles formation during the reduction of Ag^+ ions by ascorbic acid and hydrazine in presence of cationic, anionic and nonionic surfactants (Al-Thabaiti et al., 2008; Khan et al., 2009). It was observed that nature of the surfactants head group, the nature of reducing agents, pH and time are the important parameters which controlled the growth, size and shape of Ag-nanoparticles. Dekany and his co-investigators used a mixture of two reductants (hydroquinone and sodium citrate) to study the kinetics of silver nanoparticles growth in aqueous polymer solutions of poly(vinyl pyrrolidone) and PVA. Presence of two reductants and the dual behavior of citrate (reductant and stabilizer) (Lee and Meisel, 1982; Kamat et al., 1998) give systems of considerable complexity. It was, therefore, thought to be of interest to investigate the growth of silver nanoparticles by the citric acid reduction of silver(I) with a view to have an insight into the reaction mechanism. In addition, the effect of water soluble polymer, i.e., PVA was also investigated on the growth of nanoparticles. Incidentally, this study appears to be the first report on the effect of PVA on the citric acid reduction of silver(I).

2. Experimental section

2.1. Materials and instruments

Poly(vinyl alcohol) (BDH, England grade powder, 99–100% hydrolyzed), silver nitrate (99.9%, BDH), citric acid (99–100%, BDH), cetyltrimethylammonium bromide (Fluka, 98%), sodium chloride (99%, BDH) and sodium bromide (99%, BDH) were used without further purification. Stock PVA solutions were prepared by slow stepwise addition of PVA to deionized water with fast stirring to avoid the aggregation of PVA. The water used as the solvent was previously

subjected to deionization, followed by distillation in alkaline KMnO_4 . The purity of surfactant was ascertained by the absence of minima in surface tension *versus* $\log[\text{surfactant}]$ plots (Harrold, 1960). The solutions of AgNO_3 were prepared daily and stored in a dark glass bottle. UV–vis Spectrophotometer (UV-260 Shimadzu, with 1 cm quartz cuvettes), transmission electron microscope (JEOL, JEM-1011; Japan), and pH meter (Accumet, Fisher Scientific digital pH meter 910) were used to monitor the formation of silver sol, determine the size of the silver particle and pH measurements, respectively, under different experimental conditions. For TEM, samples were prepared by placing a drop of working solution on a carbon-coated standard copper grid (300 mesh) operating at 80 kV. The relative viscosities (η_r) of reaction mixture were determined in the absence and presence of PVA to get an idea about the type of complexation between CTAB and PVA by using an Ubbelohde viscometer (Wang et al., 2008).

2.2. Kinetic procedure

Requisite volumes of silver nitrate, CTAB, and PVA (if needed) were placed into three-necked reaction flask fitted with a spiral double-walled condenser (to arrest evaporation) and the contents were thermally equilibrated at the desired temperature in a constant temperature paraffin oil bath of $\pm 0.1^\circ\text{C}$ accuracy. The reaction was started by adding citric acid solution as the last component. Progress of the yellow-color silver sol formation was followed spectrophotometrically by measuring the absorbance at definite time intervals at 412 nm (λ_{max} of silver sol; *vide infra*) against blanks containing all the constituents except citric acid and PVA. *Pseudo*-first-order conditions were maintained in all kinetic runs by using an excess of $[\text{Ag}^+]$. The *pseudo*-first-order rate constants (k_{obs} , s^{-1}) were determined by using $k_{\text{obs}} = (2.303/t) \log\{(A_\infty - A_0)/(A_\infty - A_t)\}$ of the reaction with the help of a computer program, where A_t is the absorbance at time t and A_∞ is the final absorbance, with a fixed time method.

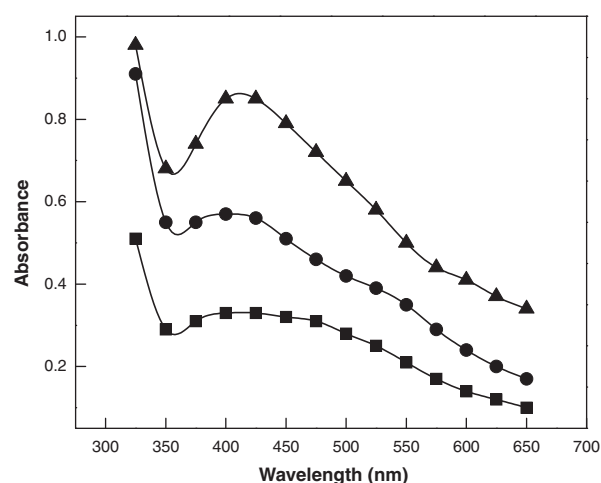


Figure 1 UV–vis absorption spectra of orange colored silver sol as a function of time. *Reactions conditions:* $[\text{citric acid}] = 4.0 \times 10^{-4} \text{ mol dm}^{-3}$; $[\text{Ag}^+] = 4.0 \times 10^{-3} \text{ mol dm}^{-3}$; $[\text{CTAB}] = 6.0 \times 10^{-4} \text{ mol dm}^{-3}$; $\text{temp.} = 23^\circ\text{C}$; $\text{time} = (\blacksquare)$ 120 min, (\bullet) 160 min and (\blacktriangle) 210 min.

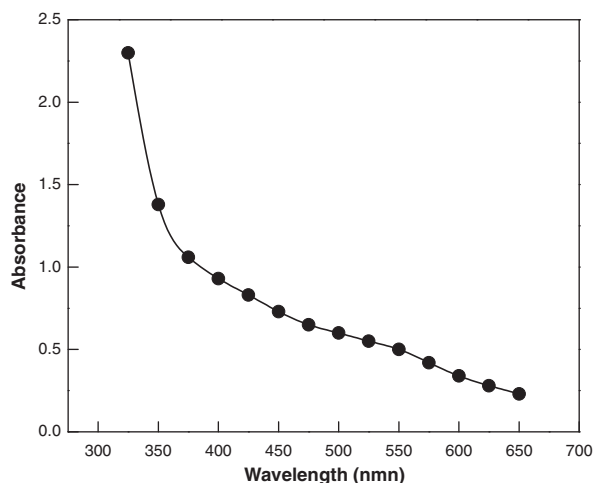


Figure 2 UV-vis absorption spectra of purple colored silver sol in presence of PVA. *Reaction conditions:* [citric acid] = 4.0×10^{-4} mol dm $^{-3}$; [Ag $^{+}$] = 4.0×10^{-3} mol dm $^{-3}$; [CTAB] = 6.0×10^{-4} mol dm $^{-3}$; [PVA] = 0.2 g dm $^{-3}$; temp. = 23 °C; time = 180 min.

3. Results and discussion

The results of the CTAB assisted silver sol formation in the reduction of silver(I) by citric acid with and without PVA are summarized as follows:

- It is well known that nature of reducing agents and pH of the working solutions are the important parameters for the formation of stable, transparent, and different colors of metal sols. The shape of the spectra gives information about the size, shape, the size distribution and the surface properties of the metal particles (Huang et al., 2006; Zhong et al., 2004). Therefore, spectra and pH of the reaction mixture ([Ag(I)] = 4.0×10^{-3} mol dm $^{-3}$, [citric acid] = 4.0×10^{-4} mol dm $^{-3}$, [CTAB] = 6.0×10^{-4} mol dm $^{-3}$) in the absence and presence of PVA (0.2 g dm $^{-3}$) were recorded at different time intervals and at the end of each kinetic experiment, respectively. The results are depicted graphically as absorbance-wavelength profiles in Figs. 1 and 2, and observed that pH drift during the course of the reaction is negligible (Table 1). Fig. 3 represents the changes in the plots of $\log(A_x - A_t)$ of citric acid-silver(I) system with definite time intervals at 23 °C in absence and presence of PVA. By inspecting Fig. 3, it is clear that the reaction has complicated kinetic features (plots of $\log(A_x - A_t)$ versus time deviate from linearity, which depends on the experimental conditions, i.e., [citric acid], [CTAB] and [Ag $^{+}$]). The time up to the linearity can be considered to be the induction period (initial slow stage). After this point, the deviation in linear plot could be called the auto-acceleration (second stage). Therefore, rate constants were determined from the slopes of the initial tangents to the plots of $\log(A_x - A_t)$ versus time (vide supra) (Khan et al., 2009).
- In the first set of experiments, a series of kinetic runs were performed to assess the role of PVA in the silver sol formation. Surprisingly, variation of [PVA] has no effect on the reaction rate ($k_{\text{obs}} \times 10^{-5} = 5.7, 5.8, 5.6, 5.9$ and 5.8 s $^{-1}$

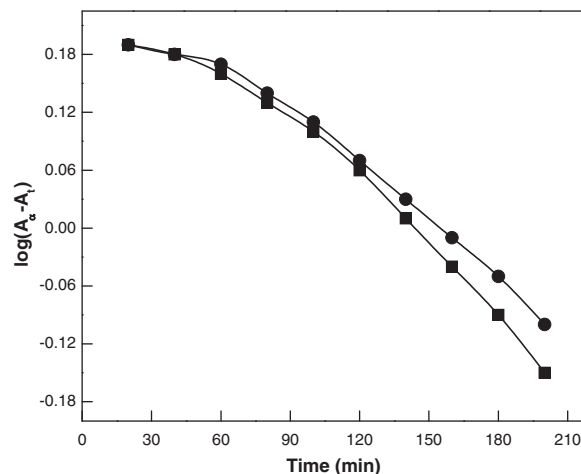


Figure 3 Plots of $\log(A_x - A_t)$ versus time in absence (●) and presence (■) of PVA at 412 nm. *Reaction conditions:* [citric acid] = 4.0×10^{-4} mol dm $^{-3}$; [Ag $^{+}$] = 4.0×10^{-3} mol dm $^{-3}$; [CTAB] = 6.0×10^{-4} mol dm $^{-3}$; temp. = 23 °C; [PVA] = 0.2 g dm $^{-3}$.

at [PVA] = 0.04, 0.08, 0.12, 0.16, and 0.20 g dm $^{-3}$, respectively) at fixed [Ag $^{+}$] (4.0×10^{-3} mol dm $^{-3}$), [CTAB] (6.0×10^{-4} mol dm $^{-3}$), [citric acid] (4.0×10^{-4} mol dm $^{-3}$), and temperature (23 °C). In the second set of experiments, the influence of [Ag $^{+}$] was studied at fixed [citric acid] (= 4.0×10^{-4} mol dm $^{-3}$), [CTAB] (= 6.0×10^{-4} mol dm $^{-3}$) and temperature (= 23 °C). The invariance of pseudo-first-order rate constants with variation in the [Ag $^{+}$] is indicative of a first-order dependence of the reaction with respect to [Ag $^{+}$] with and without PVA (Table 1). The effects of [citric acid] (range = 1.0×10^{-4} – 6.0×10^{-4} mol dm $^{-3}$) were investigated at constant [Ag $^{+}$] (= $4.0 \times$

Table 1 Effects of [citric acid], [Ag $^{+}$] and [CTAB] on the k_{obs} of silver nanoparticles formation at 412 nm.

[citric acid] ($\times 10^4$ mol dm $^{-3}$)	[Ag $^{+}$] ($\times 10^3$ mol dm $^{-3}$)	[CTAB] ($\times 10^4$ mol dm $^{-3}$)	pH	k_{obs} ($\times 10^5$ s $^{-1}$)
1.0	4.0	6.0	3.2	5.6
2.0			3.2	5.5 (3.6) ^a
3.0			3.3	5.5 (5.2)
4.0			3.1	5.7 (5.9)
5.0			3.1	5.6 (6.0)
6.0			3.0	5.4 (6.0)
4.0	3.8	6.0	3.2	5.7 (6.1)
	4.2		3.2	5.6 (6.0)
	4.4		3.2	5.7 (5.9)
	4.6		3.1	5.5 (6.0)
4.0	4.0	4.0	3.2	Yellow turbidity
		6.0	3.1	5.5 (5.5)
		8.0	3.2	5.8 (5.9)
		10.0	3.2	6.0 (6.0)
		12.0	3.1	6.1 (6.1)
		14.0	3.3	6.7 (6.1)
		16.0	3.2	7.4 (6.1)
		18.0	3.2	8.1 (6.1)

^a Values of rate constants in presence of PVA (= 0.2 g dm $^{-3}$) are given in parentheses.

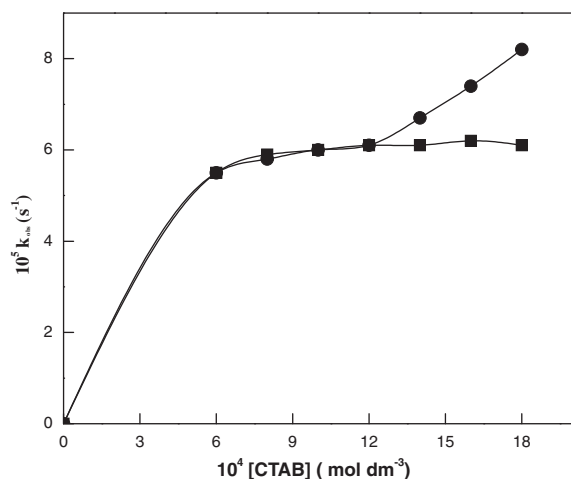


Figure 4 Effect of [CTAB] on k_{obs} of silver nanoparticles formation in absence (■) and presence (●) of PVA. *Reaction conditions:* [citric acid] = 4.0×10^{-4} mol dm $^{-3}$; [Ag $^{+}$] = 4.0×10^{-3} mol dm $^{-3}$; [CTAB] = 6.0×10^{-4} mol dm $^{-3}$; [PVA] = 0.2 g dm $^{-3}$; temp. = 23 °C.

10^{-3} mol dm $^{-3}$), [CTAB] ($=6.0 \times 10^{-4}$ mol dm $^{-3}$) and temperature ($=23$ °C). The pseudo-first-order rate constants were found to be independent on the initial concentrations of citric acid in both media (Table 1) indicating the order to be one with respect to [citric acid].

3. Micellar pseudo-phase is regarded as a microenvironment having varying degree of water activity, polarity and hydrophobicity. The micelle is a porous cluster with deep-water-filled cavities. The water activity is slightly lower at the interface than in the bulk due to the high ionic concentration in the micellar region (Bunton, 1997). The location of the reactants and the degree of water penetration into the micellar structure have major influence on reactivity. Therefore, the effect of [CTAB] ($=4.0 \times 10^{-4}$ – 18.0×10^{-4} mol dm $^{-3}$) was studied at constant [Ag $^{+}$] ($=4.0 \times 10^{-3}$ mol dm $^{-3}$), [citric acid] ($=4.0 \times 10^{-4}$ mol dm $^{-3}$) and temperature ($=23$ °C). The k_{obs} –[CTAB] profile shows increase in the rate constants with increase [CTAB] (Fig. 4; (●)) at

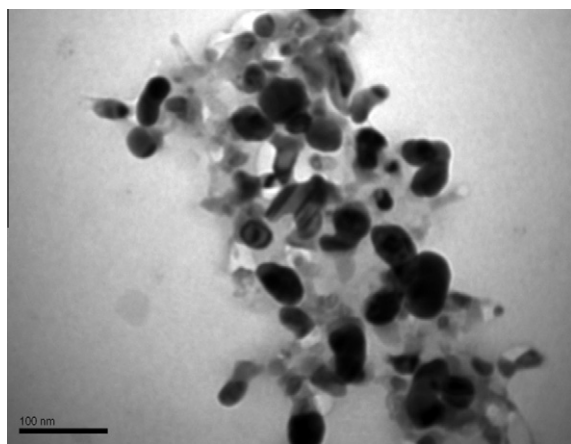


Figure 5 TEM images of silver nanoparticles. *Reaction conditions:* [citric acid] = 4.0×10^{-4} mol dm $^{-3}$; [Ag $^{+}$] = 4.0×10^{-3} mol dm $^{-3}$; [CTAB] = 6.0×10^{-4} mol dm $^{-3}$; temp. = 23 °C.

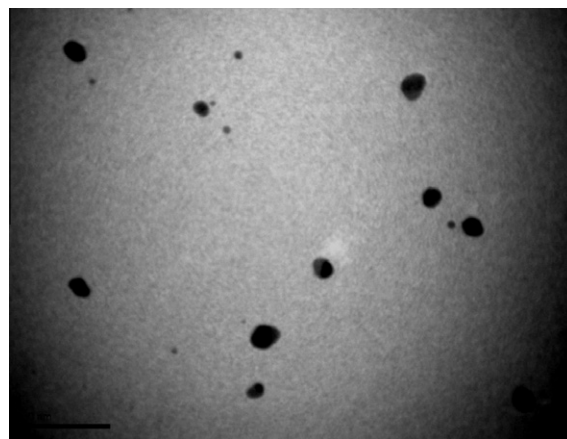


Figure 6 TEM images of silver nanoparticles in presence of PVA. *Reaction conditions:* [citric acid] = 4.0×10^{-4} mol dm $^{-3}$; [Ag $^{+}$] = 4.0×10^{-3} mol dm $^{-3}$; [CTAB] = 6.0×10^{-4} mol dm $^{-3}$; [PVA] = 0.2 g dm $^{-3}$; temp. = 23 °C.

constant [PVA]. This may be attributed to solubilization/incorporation of the reactant species and/or silver particles into the micellar phase and adsorption of silver particles on the surface of CTAB micelles. Thus, we may safely conclude that both reactants (citric acid and silver(I)) are distributed among the different pseudo-phases present in the reaction mixture (Khan and Talib, 2010). Interestingly, the variation of [CTAB] has no significant effect on the reaction rate in absence of PVA (■).

4. The shape, size, and the size distribution CTAB-stabilized silver nanoparticles were determined with the help of transmission electron microscope (TEM). In a typical experiment, 20.0 cm 3 of 0.01 mol dm $^{-3}$ AgNO $_3$, 3.0 cm 3 of 0.01 mol dm $^{-3}$ CTAB with citric acid (2.0 cm 3 of 0.01 mol dm $^{-3}$) was made to a total vol of 50 cm 3 at 25 °C. Figs. 5 and 6 show the TEM pictures observed after adding the citric acid in absence and presence of PVA, respectively. The electron microscopy pictures show the different behavior of PVA in the formation of silver nanoparticles having different morphologies.
5. The association between ionic micelles and polymers usually leads to a stabilization of the micelles, which is apparent from the reduced value of the critical micelle concentration. Surfactant–polymer interaction depends on both the relative charge and the hydrophobicity of the

Table 2 Relative viscosities (η_r) of reaction mixtures at different [PVA].^a

[PVA] ($\times 10^2$ g dm $^{-3}$)	η_r
0.0	1.00
2.0	1.10
5.0	1.11
8.0	1.09
12.0	1.12
150.0	1.11

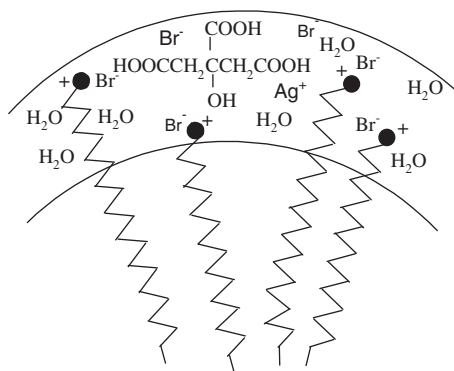
^a [Ag(I)] = 4.0×10^{-3} mol dm $^{-3}$; [CTAB] = 6.0×10^{-4} mol dm $^{-3}$; temp. = 23 °C; [citric acid] = 4.0×10^{-4} mol dm $^{-3}$.

surfactant–polymer pair. Increasing of the surfactant concentration leads to a saturation of the polymer domain, and finally free micelles in solution will coexist with aggregates supported on the polymer backbone (Brackman and Engberts, 1991). Therefore, in order to see the interactions between CTAB and PVA, the relative viscosity of the CTAB–PVA reaction mixtures were determined under different experiment conditions. No appreciable change of η_r was observed with increasing [PVA] at constant [CTAB] (Table 2) indicating no strong evidence for the complexation between CTAB and PVA.

The effect of PVA on the silver nanoparticles formation was studied under the similar experimental conditions of $[\text{Ag}^+]$, [citric acid], and [CTAB] to those employed in the absence of PVA. It was observed that reaction follows the same order kinetics (vide supra) with respect to $[\text{Ag}^+]$ and [citric acid]. These results undoubtedly show that the reaction mechanism and rate-law in the presence of PVA remains the same as that in the CTAB homogeneous aqueous media. Taking into account the nature of silver sol, interestingly, it is to be noted that nature (λ_{max} and position) of the plasmon absorption band, colors, shape, and size of the colloidal silver sols depend on the method of preparation, presence of additives (polymers and nucleophiles), and state of aggregation (Henglein, 1993; Sondi et al., 2003; Zhai and Efrima, 1996; Suber et al., 2005). The experimental finding is that our spectra of yellow-color silver sol consist one broad plasmon band with $\lambda_{\text{max}} = 412 \text{ nm}$ (Fig. 1), while in presence of PVA, purple color appeared, spectra of this sol cover the whole visible region of the spectrum (Fig. 2). The change in the shape of the spectrum provides clear evidence for the adsorption of PVA on the silver particles. These observations are in good agreement with the results of Henglein (1993) (neutral polymers strongly influence the plasmon absorption band of silver metal particles via lone pairs of electrons).

The TEM images in Fig. 5 indicate that the sphere-shaped and differently sized silver nanoparticles were prepared under our experimental conditions. On the other hand we do not find such type of aggregation with PVA (Fig. 6). However, the silver nanoparticles are spherical and of different particle size having irregular distribution. These findings also suggest that the PVA strongly adsorbed on the surface of particles which totally suppress the particle aggregation.

The influence of [CTAB] on the rate of silver nanoparticles formation is shown in Table 1. It has been found that for [CTAB] lower than $6.0 \times 10^{-4} \text{ mol dm}^{-3}$ no kinetic effects are observed due to the appearance of yellow precipitate. Above this concentration, the reaction rate increases by increasing [CTAB] observed, in agreement with the incorporation and/or solubilization of the citric acid and silver(I) into the micelles (at low surfactant concentration the normal micelle is spherical). Micellar surfaces are water rich and do not provide a uniform reaction medium because micelle is a porous cluster with a rough surface and deep-water-filled cavities. Polarity and water content in different regions of the micelle (Gouy–Chapman-, Stern-, and palisade-layer) play an important role in the rate of reaction in these regions (Bunton et al., 1991; Tascioglu, 1996; Cerichelli et al., 1994). The micelles assisted reactions are believed to occur in the Stern layer (Khan and Talib, 2010). Citric acid gets incorporated into the palisade layer with the three $-\text{COOH}$ groups



Scheme 1 Solubilization of reactants in the micellar *pseudo*-phase of CTAB micelles.

remaining in the Stern layer of the CTAB micelles. The presence of Ag^+ in the Stern layer (water rich region) can not be ruled out. As a result, CTAB micelles help in bringing the both reactants closer, which may orient in a manner suitable for the electron transfer (Scheme 1).

It is interesting to note that the reaction rate is not affected significantly by the presence of PVA (Table 1). Our results seem to suggest that there is a competition between citric acid and PVA to solubilize and/or incorporate into the Stern layer by electrostatic or chemical forces. The hydrophobic moiety ($-\text{CH}_2\text{CH}(\text{OH})\text{CH}_2-$) of citric acid prevent the solubilization of PVA, rules out the exclusion of solubilized citric acid from the reaction site. On the other hand, different shape of UV–vis spectra indicates that adsorption of PVA on the surface of silver nanoparticles. In addition changes in the morphologies of the nanoparticles are taken into account for the differential TME images (Figs. 5 and 6).

The pH values was found to be nearly constant with increasing [CTAB] and [citric acid] (weak acid; $K_{a1} = 7.10 \times 10^{-4}$; $K_{a2} = 1.68 \times 10^{-5}$; $K_{a3} = 6.0 \times 10^{-6}$). The observed values of pH are given in Table 1. In aqueous solution, various citric acid species exist in equilibrium and nature of these species depends upon the pH of the working solution. Under our experimental conditions (Table 1), the neutral form of citric acid is the major and reactive species. On the basis of above results and previous observations (Khan and Talib, 2010; Malik et al., 2010), Scheme 2 has been proposed for the silver nanoparticles formation.

In Scheme 2, Eqs. (1)–(3) represents, respectively, the ionization of citric acid. By analogy with the previous results (Al-Thabaiti et al., 2008; Khan et al., 2009; Khan and Talib, 2010; Malik et al., 2010) we assume that Eq. (4) is the rate determining step of the reaction studied (one-step one-electron oxidation–reduction mechanism) to yield Ag^0 and radical.

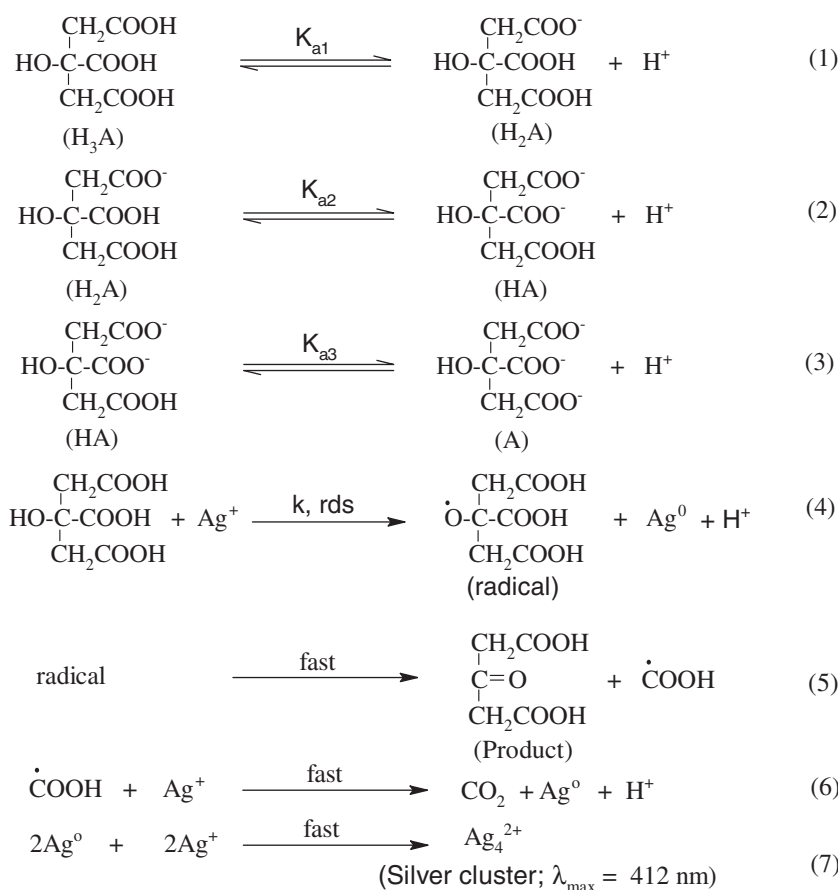
The rate of silver sol formation, in terms of Scheme 2 is given by Eq. (8):

$$\frac{d[\text{silver sol}]}{dt} = \frac{k[\text{H}^+][\text{Ag}^+][\text{citric acid}]_T}{[\text{H}^+] + K_{a1}} \quad (8)$$

The inequality $[\text{H}^+] \gg K_{a1}$ is evident under our experimental conditions (Table 1), and the rate-law, Eq. (8), then reduces to Eq. (9):

$$\frac{d[\text{silver sol}]}{dt} = k[\text{Ag}^+][\text{citric acid}]_T \quad (9)$$

and for the first-order rate constants:



Scheme 2 Mechanism for the reduction of Ag^+ to Ag^0 by citric acid.

$$k_{\text{obs}} = k[\text{Ag}^+] \quad (10)$$

Eq. (8) is in good agreement with the experimental results obtained at constant pH, since kinetic orders in $[\text{Ag}^+]$ and [citric acid] are all unity.

4. Conclusions

The most interesting feature of this study is the adsorption of silver nanoparticles into the larger particles. We are unaware of any precedence in the kinetics of aggregated silver particles formation. It has been observed that the presence of PVA strongly inhibits the adsorption and/or aggregation of particles. Though the data are not conclusive, it seems that presence of polymer chains prevents these processes due to steric effect. This gives an indication to the relationship between the lone-pairs of electrons of PVA and the surface of the silver particles.

Acknowledgment

The financial support to the authors by Deanship of Scientific Research (430/071-3), King Abdul Aziz University, is gratefully acknowledged.

Appendix A. Derivation of rate equation

From Scheme 2,

$$\frac{d[\text{silver sol}]}{dt} = k[\text{Ag}^+][\text{H}_3\text{A}] \quad (\text{A1})$$

$$K_{a1} = \frac{[\text{H}_2\text{A}][\text{H}^+]}{[\text{H}_3\text{A}]}$$

$$[\text{H}_2\text{A}] = \frac{K_{a1}[\text{H}_3\text{A}]}{[\text{H}^+]} \quad (\text{A2})$$

The total [citric acid] under our experimental conditions (pH 3.3) is given by

$$\begin{aligned}
 [\text{citric acid}]_{\text{T}} &= [\text{H}_3\text{A}] + [\text{H}_2\text{A}] \\
 &= [\text{H}_3\text{A}] + \frac{K_{a1}[\text{H}_3\text{A}]}{[\text{H}^+]} \\
 [\text{H}_3\text{A}] &= \frac{[\text{citric acid}]_{\text{T}}[\text{H}^+]}{([\text{H}^+] + K_{a1})} \quad (\text{A3})
 \end{aligned}$$

Substituting the value of $[\text{H}_3\text{A}]$ in Eq. (A1), we get

$$\frac{d[\text{silver sol}]}{dt} = \frac{k[\text{H}^+][\text{Ag}^+][\text{citric acid}]_{\text{T}}}{[\text{H}^+] + K_{a1}} \quad (6)$$

References

- Al-Thabaiti, S.A., Al-Nawaiser, F.M., Obaid, A.Y., Al-Youbi, A.O., Khan, Z., 2008. *Colloid Surf. B: Biointerf.* 67, 230.
- Bakar, N.H.H.A., Ismail, J., Bakar, M.A., 2007. *Mater. Chem. Phys.* 104, 276.
- Ball, P., 1991. *Nature* 349, 101.
- Brackman, J.C., Engberts, J.B.F.N., 1991. *Langmuir* 7, 2097.
- Bunton, C.A., 1997. *J. Mol. Liq.* 72, 231.
- Bunton, C.A., Nome, F., Romsted, L.S., Quina, F.H., 1991. *Acc. Chem. Res.* 24, 357.
- Cerichelli, G., Mancini, G., Luchetti, L., Savelli, G., Bunton, C.A., 1994. *Langmuir* 10, 3982.
- Henglein, A., 1998. *Chem. Mater.* 10, 444.
- Harrold, S.P., 1960. *J. Colloid Sci.* 15, 280.
- Henglein, A., 1993. *J. Phys. Chem.* 97, 5457.
- Huang, H.H., Ni, X., Loy, G.L., Chew, C.H., Tan, K.L., Loh, F.C., Deng, J.F., Xu, G.Q., 1996. *Langmuir* 12, 909.
- Huang, Y.F., Huang, K.M., Chang, H.T., 2006. *J. Colloid Interf. Sci.* 301, 145.
- Jana, N.R., Sau, T.K., Pal, T., 1999. *J. Phys. Chem. B* 103, 115.
- Kamat, P.V., Flumiani, M., Hartiand, G.V., 1998. *J. Phys. Chem.* 102, 3123.
- Keki, S., Torok, J., Deak, G., Daroczi, L., Zsuga, M., 2000. *J. Colloid Interf. Sci.* 229, 550.
- Khan, Z., Talib, A., 2010. *Colloid Surf. B: Biointerf.* 76, 164.
- Khan, Z., Al-Thabaiti, S.A., El-Mossalamy, E.H., Obaid, A.Y., 2009. *Colloid Surf. B: Biointerf.* 73, 284.
- Kim, M., Byun, J.-W., Shin, D.-S., Lee, Y.-S., 2009. *Mater. Res. Bull.* 44, 334.
- Lee, P.C., Meisel, D., 1982. *J. Phys. Chem.* 86, 3391.
- Lee, M.-H., Oh, S.-G., Suh, K.-D., Kim, D.-G., Sohn, D., 2002. *Colloid Surf. A* 210, 49.
- Malik, M.A., El-Nowaiser, F.M., Ahmad, N., Khan, Z., 2010. *Int. J. Chem. Kinet.* 42, 704.
- Mayer, A.B.R., Hausner, S.H., Mark, J.E., 2000. *Polym. J.* 32, 15.
- Pal, T., Sau, T.K., Jana, N.R., 1997. *Langmuir* 13, 1481.
- Patakfalvi, R., Viranyl, Z., Dekany, I., 2004. *Colloid Polym. Sci.* 283, 299.
- Pileni, M.P., 1993. *J. Phys. Chem.* 97, 6961.
- Saito, R., Okamura, S., Ishizu, K., 1996. *Polymer* 37, 5255.
- Sondi, I., Goia, D.V., Matijevic, E., 2003. *J. Colloid Interf. Sci.* 260, 75.
- Suber, L., Sondi, I., Matijevic, E., Goia, D.V., 2005. *J. Colloid Interf. Sci.* 288, 489.
- Tascioglu, S., 1996. *Tetrahedron* 52, 11113.
- Wang, W., Chen, X., Efrima, S., 1999. *J. Phys. Chem. B* 103, 7238.
- Wang, W., Wang, J., Sun, P., Yuan, Z., Ding, D., Chen, T., 2008. *Mater. Lett.* 62, 711.
- Zhai, X., Efrima, S., 1996. *J. Phys. Chem.* 100, 10235, 11019.
- Zhong, Z., Patskovskyy, S., Buovrette, P., Lung, J.H.T., Gedanken, A., 2004. *J. Phys. Chem. B* 108, 4046.